Algal Research 90 (2025) 104211

Contents lists available at ScienceDirect

Algal Research

journal homepage: www.elsevier.com/locate/algal

Continuous process for manoyl-oxide production and in-situ extraction from microalgae cultures

Josué M. Heinrich [a,*], Iago Teles Dominguez Cabanelas [a], Sara S. Cidraes Vieira [a], Rafael García-Cubero [a], María J. Barbosa [a], René H. Wijffels [a,b]

[a] Wageningen University, Bioprocess Engineering, AlgaePARC, P.O. Box 16, 6700 AA Wageningen, the Netherlands
[b] Nord University, Faculty of Biosciences and Aquaculture, N-8049 Bodø, Norway

ARTICLE INFO

Keywords:
Microalgae
Diterpenes
In-situ extraction
Process intensification
Genetic engineering

ABSTRACT

Eukaryotic green microalgae hold potential as green-cell factories for the production of heterologous compounds such diterpenes. Previously, a *C. reinhardtii* UVM4 strain was genetically modified to express heterologous diterpene synthases (diTPSs) and the enzymes participating in the 2-*C*-methyl-D-erythritol 4-phosphate (MEP) pathway. In this work, bench-scale continuous production of manoyl oxide (MO) was performed to prove the technical feasibility of the production system and to estimate the MO production rates. Furthermore, the influence of the operational conditions like biomass concentration, light availability, and the extraction capacity on the MO productivity was assessed.

In this work, we showed that it is possible to continuously produce/extract of manoyl oxide from a genetically engineered *C. reinhardtii* cultures in bench-scale photobioreactors, producing up to 6.7 mg l^{-1} d^{-1}. Next, we analyze the influence of the culture conditions on the biomass and manoyl oxide production rates. We found that increasing the light intensity enhances manoyl oxide production but, if diterpenes are not efficiently extracted from the culture, the MO production is significantly hindered, decreasing 7.5 times in relation to the maximum production rate. From our experimental results, we conclude that the extraction capacity is one of the most important factors affecting the efficiency of MO production in microalgal cultures and, if the extraction process is not efficient, increasing the light availability in the culture has a minor impact on the MO productivity.

1. Introduction

Isoprenoids (also known as terpenes or terpenoids) are a large family of chemical compounds exhibiting an enormous variety in terms of structural and functional properties. Because of this diversity, they can take part in a wide range of biological functions: from photosynthesis to plant defense and signaling and membrane constituents [1]. Besides their natural functions, some isoprenoids are also economically interesting, as they might be used in the production of medicines, food additives, biocontrol agents, cosmetics, chemical building blocks, and biofuels [2,3].

Although high-value isoprenoids can be obtained from their natural source (mainly from the plant *Salvia sclarea*), their industrial production is expensive [4]. As an alternative, the production of heterologous isoprenoids using genetically modified fermentative microorganisms like yeast and bacteria is also possible and shows several economic advantages [26]. In addition, biological synthesis is preferred over chemical synthesis because the last might display low yields and different stereospecific orientations of the functional groups [5]. Lauersen et al. (2018) [6] demonstrated that *C. reinhardtii* cells have a remarkable potential for heterologous production of non-native isoprenoids. In that work, the diterpenoids casbene, taxadiene, and 13R(+) manoyl oxide were produced after expressing heterologous diterpene synthases and enzymes participating in the 2-*C*-methyl-D-erythritol 4-phosphate (MEP) pathway. From lab scale experiments, it was concluded that microalgae might hold enormous potential as green-cell factories for the production of diterpenoids. Nevertheless, additional results at bench scale photobioreactors are required to prove the techno-economic feasibility of this technology.

Biomass cultivation is the starting point for the commercialization of industrial products from algae. When the desired product needs to be isolated from other cellular components, after cell density achieves the desired concentration, downstream process stages should follow. Downstream processing could involve harvesting, cellular disruption,

* Corresponding author at: Wageningen University, Bioprocess Engineering, AlgaePARC, P.O. Box 16, 6700 AA Wageningen, the Netherlands.
E-mail address: josue.heinrich@wur.nl (J.M. Heinrich).

https://doi.org/10.1016/j.algal.2025.104211
Received 9 December 2024; Received in revised form 5 July 2025; Accepted 11 July 2025
Available online 22 July 2025

product extraction, and solvent recovery. These processes, in general, imply high energy-consuming steps, which directly impact the final cost of the product [7]. Biomass disruption is not only expensive but also brings associated to it, the necessity of producing high volumes of microalgae, demanding large photobioreactor volumes, and high costs associated with nutrient usage and energy consumption for biomass cultivation [8]. To avoid expensive downstream processes, the use of a "milking" process for in-situ extraction of compounds from microalgae has been assessed [9,10]. Milking is a cultivation method that allows the simultaneous production and extraction of hydrophobic compounds from cell suspensions. It involves a two-phase bioreactor containing an aqueous phase and an organic solvent phase. Cells are cultivated in the aqueous phase, where they produce the target lipophilic compound. This compound is extracted from the cells to an organic phase in contact with the culture in a continuous process. The milking approach becomes particularly relevant in the case of isoprenoids, as many—especially smaller molecules like manoyl oxide—can diffuse freely across the cell membrane into the aqueous phase, from which they must be efficiently removed. In this context, in situ extraction offers both technical and economic advantages by enabling continuous product removal and potentially reducing downstream processing costs. In situ extraction has great potential but can be limited in practice due to undesired side effects [11]. Depending on the solvent choice, cells may be disrupted, leading to membrane destabilization and lysis, which affects cell growth. Additionally, emulsions can form during the extraction of lipophilic and amphipathic compounds, negatively impacting both cell propagation and downstream processing [12]. Continuous extraction, or "milking," is particularly important if the accumulation of the product is inhibitory which could drastically reduce the overall productivity. [6].

The aim of this research was to study a potential process to produce and extract manoyl oxide (MO) from a genetically engineered *C. reinhardtii* strain in bench scale photobioreactors cultures. Three different experimental set ups were used to analyze the effect of the light intensity on biomass and manoyl oxide production rates. In the first set of experiments, the effect of light intensity on manoyl oxide production was assessed in Erlenmeyer flasks culture (Algaebator). Results showed no significant differences in terms of growth and manoyl oxide production when high and low light conditions were compared. In a second set of experiments, the process was scaled up to a 1.8 l flat panel photobioreactor (Infors) under turbidostat control and included an external extraction system for continuous diterpene extraction. Since manoyl oxide productivities in the Infors system underperformed all Erlenmeyer cultures, a third set of experiments was performed in a 400 ml flat panel photobioreactor (Algaemist) to investigate the influence of the MO extraction capacity on the MO productivity. From all these experiments, we can conclude that though light availability influences MO productivities, the extraction capacity of the system needs to be optimized to achieve efficient production processes.

2. Materials and methods

2.1. Microalgae strain and inoculum

Chlamydomonas reinhardtii (B2) was gently provided by Kyle Lauersen (Lauersen et al. 2018). *C. reinhardtii* (B2) was genetically modified to produce 13R(+) manoyl oxide after expressing heterologous diterpene synthases and enzymes participating in the 2-*C*-methyl-D-erythritol 4-phosphate (MEP). For cell maintenance and inoculum production, microalgae were grown in 250 ml Erlenmeyers containing 100 ml of Tris-Acetate-Phosphate (TAP) Medium [13]. Cultures were kept in a shake incubator at 25 °C with 0.2 % CO_2 and 150 μmol m^{-2} s^{-1} of light intensity in a 16 h:8 h day-night cycle.

2.2. Algaebator experiments

Algaebator (Workshop Wageningen University, The Netherlands) is an incubator chamber designed for microalgal cultivations. In this system, microalgae are grown in 250 ml Erlenmeyer flasks with 100 ml of T2P 2 N medium. Mixing is achieved through agitation at the bottom of the flask using a magnetic stirrer. Initially, cultures were illuminated 24 h with a light intensity of 150 μmol m^{-2} s^{-1} for two days. After one day of culture, a 10 ml of extraction solvent (dodecane) overlaye was added to the flasks. After two days of culture, the light was increased to 318 or 636 μmol_{PAR} s^{-1} m^{-2} for the low or high light conditions, respectively. Samples were taken daily for biomass and MO determinations. The contact area between the aqueous and dodecane phase in these experiments was 90.8 cm^2.

2.3. Infors experiments

Microalgae were grown in 1.8 l Infors flat panel photobioreactors [14]. Temperature was set at 25 °C, pH set-point was 7.2, an airflow of 1 LPM enriched with 2 % CO_2 and a 16 h:8 h day-night cycle was established. Cultures were grown in T2P 2 N medium, a TAP modified medium with 2× phosphate and nitrogen concentrations [15]. After sterilization, the reactor was filled with sterilized medium and inoculated at an optical density of 0.05 (λ = 750 nm), equivalent to a biomass concentration of 23 mg l^{-1}. Cultures were grown in batch mode until stationary phase was reached. Immediately afterwards, the photobioreactor was shifted to turbidostat control. It was considered that the culture achieved a steady state, when the same biomass concentration was determined for, at least, a period of 3 residence times. During the batch operation phase, light intensity was gradually increased, from 50 μmol m^{-2} s^{-1} to the final intensities used in each experiment (Table 2). The photobioreactor illuminated area was 0.047 m^2. Once a steady state was reached, the culture was recirculated constantly between the photobioreactor and an extraction vessel by means of a peristaltic pump (Watson-Marlow multi-channel peristaltic pump was used, model 205 U, 15.3 ml min^{-1}). The extraction vessel consisted in a 500 ml Schott flask containing 200 ml of culture and 100 ml of extraction solvent (dodecane) (Fig. 1). The contact area between the aqueous and dodecane phases was 33.7 cm^2.

Biomass concentration, CO_2 availability, and the PFD (Photon Flux Density, μmol_{PAR} m^{-2} s^{-1}) were kept constant during the cultivation period. Both nutrients concentration in aqueous and extraction phase (dodecane) were assumed constant during each run for calculation purposes despite daily sampling. This assumption was based on the fact that sample volumes could be considered irrelevant (<1 ml) when compared to the dodecane volume in the extraction vessel.

2.4. Algaemist experiments

Similar to infors cultivations, microalgae were grown in a turbidostat mode in a 400 ml flat panel photobioreactor named Algaemist (Workshop Wageningen University, The Netherlands) [16]. Culture conditions, experimental setup and procedures were the same as in Infors reactor experiments. Light intensities selected and biomass concentrations achieved in each steady state were different in each experiment (Table 3). The illuminated area of the Algaemist photobioreactors was 0.028 m^2. However, in these experiments, the extraction vessel consisted in a 250 ml Schott flask containing 100 ml of culture and 50 ml of extraction solvent (dodecane). The contact area between the aqueous and dodecane phases in these experiments was 23.8 cm^2.

2.5. Biomass concentration

Culture growth was determined by optical density (λ = 750 nm) and dry weight measurements. Briefly, a sample of culture was filtered through pre-dried (100 °C overnight) and pre-weight Whatman glass fiber filter (GF/F; Whatman International Ltd., Maidstone, UK). After the filtration, the glass fiber filter containing the microalgal biomass from the sample was dried overnight at 100 °C and cooled down at room

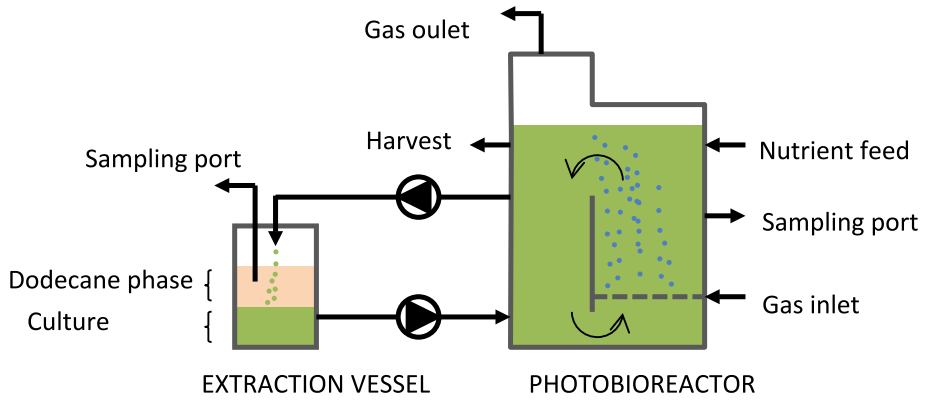

Fig. 1. Experimental set-up used to continuously produce and extract MO from *C. reinhardtii* (B2).

temperature right before weighing. The following correlation (Eq. (1)) between the OD_{750nm} and the biomass concentration was established ($R^2 = 0.993$):

$$\text{Biomass concentration}\left(gL^{-1}\right) = 0.4592 \bullet OD_{750\ nm}. \quad (1)$$

2.6. Manoyl oxide concentration

The concentration of each sample (200 μl) containing manoyl oxide (MO) in the dodecane phase was determined using a GC-FID 7890A from Agilent using a RESTEK Rxi-5 ms column 0.25 μm (5 % diphenyl, 95 % dimethylpolysiloxane). The calibration curve was performed by means of a set of standard samples with a known concentration of manoyl oxide (100-50-25-10-5 mg l^{-1}) (Sigma-Aldrich) and correlating them with the peak's area shown in the GC-FID chromatogram [15]. The temperature of the injector was 250 °C, a constant flow of 1 ml min^{-1} of hydrogen at 18.139 kPA was used as a carrier gas. The oven temperature was held at 50 °C for 0.45 min, then raised to 120 °C at 22.04 °C min^{-1}, followed by 6.61 °C min^{-1} to 160 °C, later to 270 °C at 22.04 °C min^{-1} which was held for 1 min. Finally, temperature was raised to 320 °C at 22.04 °C min^{-1} and held for 5 min. The detector temperature was placed at 325 °C. Areas of peaks with retention time related to manoyl oxide were then determined using the calibration curve.

3. Results and discussion

3.1. Preliminary experiments in Erlenmeyer flasks, Algaebator

This work started by reviewing the available information on the strain, which was developed and tested by Lauersen et al. [6]. Their results showed that a genetically modified *Chlamydomonas reinhardtii* strain (named as strain B2) can produce manoyl oxide (MO). In those experiments, a MO productivity of 7.14 mg l^{-1} d^{-1} was accomplished, using 16 h:8 h day:night cycles and CO_2 as the sole carbon source (Table 1). The produced MO was extracted in situ by a dodecane overlayer in contact with the broth. Because of the high hydrophobicity of MO, it is assumed that it will be moved from intracellular membranes into the dodecane overlay, where it accumulates throughout the process. Another important conclusion drawn from the experimental data in Laeursen et al. is that MO production stops if the diterpene is not extracted from the culture media (i.e., product inhibition). On the other hand, when microalgae were grown without solvent (dodecane) in the culture, the amount of MO produced decreased 30,000 times compared to experiments under the same conditions but with dodecane (Table 1). The results of these experiments were used as a starting point to design the experiments of the current work.

Table 1
MO titers for cultures with (DD+) or without (DD−) dodecane from the work of Lauersen et al. (2018).

Culture parameter	Units	DD+	DD-
Dodecane volume	[ml]	0.5	0
Culture volume	[ml]	4.5	4.5
Biomass concentration	[g l^{-1}]	0.050	0.099
Cell count	[cell ml^{-1}]	3.53E+07	3.84E+07
MO conc. in the Biomass	[mg g^{-1}]	0.036	0.050
MO conc. in the culture medium	[mg l^{-1}]	0.015	0.039
MO conc. in the dodecane	[mg l_{DD}^{-1}]	40.647	–
Total MO produced	[μg]	20.6	6.24×10^{-4}

Although the results described above show that *C. reinhardtii* B2 might produce MO, it is not described how the culture conditions and, specially, light availability might affect the MO production rate. In the current work, we aimed to analyze how MO productivity and extraction rates are influenced by light intensity.

The influence of light availability was first analyzed in the Algaebator. Cells of *C. reinhardtii* grown in Erlenmeyers, were exposed to two different light intensities: 318 (Low light intensity, L_D) and 636 (High light intensity, H_D) μmol m^{-2} s^{-1} (Fig. 2).

Our results suggest that increasing light availability displays a minor impact on MO production (Fig. 2). Under low light conditions (318 μmol m^{-2} s^{-1}), average biomass and MO productivities were 0.33 ± 0.06 g l^{-1} d^{-1} and 6.2 ± 0.5 mg l^{-1} d^{-1}, respectively. Both results, obtained at different light intensities, are similar to the previous reported by Lauersen [6]. When the photon radiation flux was doubled (from 318 to 636 μmol m^{-2} s^{-1}), biomass and MO productivities remained the same, with values of 0.30 ± 0.06 g l^{-1} d^{-1} and 6.7 ± 0.6 mg l^{-1} d^{-1} respectively. *Chlamydomonas* species can withstand high light intensities [17]. Both high and low conditions led to the maximum biomass production at the same time, leading to similar productivity. The reason for the lack of a difference could be due to light saturation. This is a common phenomenon in microalgae cultivation [18,19] and would explain why doubling the photon radiation flux showed little effect on productivity. Another possible explanation could be limited aeration in the flasks, resulting in reduced CO_2 availability. For this reason, we proposed to scale up the process to 3 l and continue the investigation in thin flat panel reactors (Infors: 2 cm depth cultivation chamber), where light penetration wouldn't be an issue even for the highest biomass densities.

3.2. Continuous production of MO in bench scale photobioreactor

Using light and CO_2, microalgae can produce MO inside the chloroplasts and, to reach the dodecane phase, diterpene molecules need to be excreted from cells into the culture medium and then extracted into the organic phase. The cellular mechanism for the extraction of non-polar intracellular metabolites in bilayer bioreactor systems is still not completely understood [11,20]. However, considering the experimental results from the current and previous research, we propose a mechanism consisting in three steps: (1) compounds are produced inside the cells,

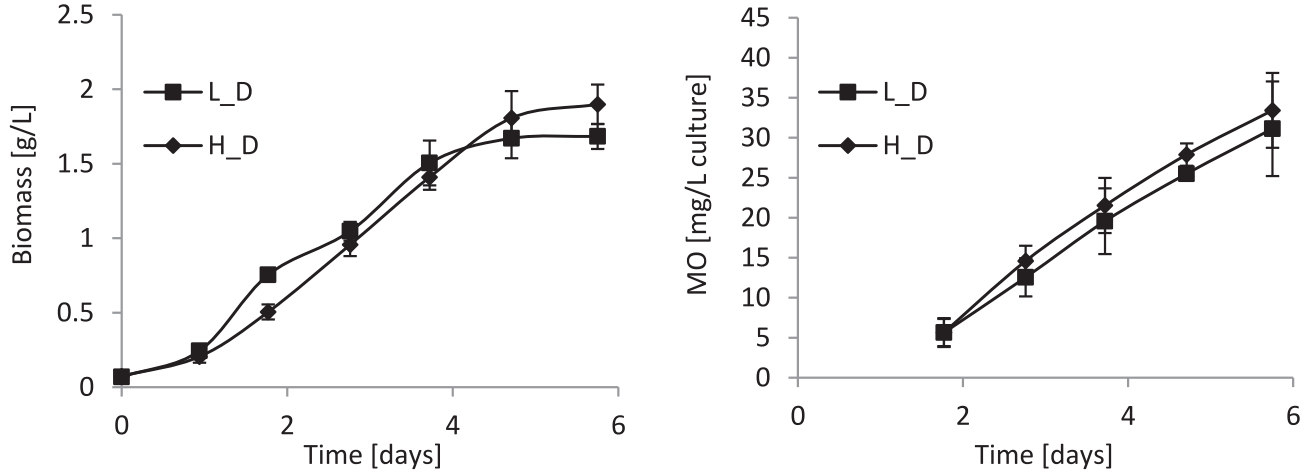

Fig. 2. Biomass (a) and MO (b) concentrations over time for cultures under High light intensity (H_D) and Low light intensity (L_D).

(2) from the intracellular space they diffuse to the culture media, after which, (3) they are extracted into the organic phase by a liquid-liquid extraction process (Fig. 3).

To demonstrate the feasibility of continuous heterologous production and extraction of diterpenes from genetically modified microalgae, *C. reinhardtii* B2 strain was cultured in a flat-panel Infors photobioreactor under turbidostat control with a constant PFD (photon flux density) of 636 μmol m^{-2} s^{-1}. This PFD was selected based on previous work [14]. Light intensity simulated the average outdoors light regime of 3 summer months (June, July, and August) for the last ten years at AlgaePARC (51°59′44.1″N 5°39′26.2″E) using the European Photovoltaic Geographical Information System (PVGIS). Details of the experimental set up can be seen in Fig. 1. Different turbidostats experiments were done, at different biomass concentrations: 0.79, 1.37, and 2.32 g l^{-1} (Table 3). A fourth experiment was included using a PFD of 1877 μmol m^{-2} s^{-1} and a biomass concentration of 2.01 g l^{-1} in order to assess the performance under high light intensity [21]. The different PFD and biomass concentrations allowed different ratios of light/cell, i.e., the ratio between the PFD and the biomass concentration (Eq. (6)).

In a photobioreactor operated under turbidostat control, fresh media is continuously added to the bioreactor to compensate microalgae growth keeping the biomass concentration constant [22]. To avoid changes in the reactor volume, the same amount of media must be harvested from the reactor vessel. In this scenario, the total amount of MO produced in the photobioreactor will be divided into three fractions: the amount of MO extracted in the dodecane phase and the amount of MO that leaves the bioreactor through the harvest (thus, inside the cells and in the aqueous phase) (Fig. 3).

From the mass balances for the microalgae biomass and manoyl oxide in each phase, the following differential equations system emerges (Eqs. (1) to (4)).

$$\mu_x = \frac{Q}{V_R} \tag{1}$$

$$\frac{dm_{MO}^{DD}}{dt} = \frac{V_R}{V_{DD}}\ K_T\ m_{MO}^{AQ} \tag{2}$$

$$\frac{dm_{MO}^{AQ}}{dt} = -\frac{Q}{V_R}m_{MO}^{AQ} - \frac{Q}{V_R}\ x\ m_{MO}^{X} - K_T\ m_{MO}^{AQ} + r_{EX} \tag{3}$$

$$\frac{dm_{MO}^{X}}{dt} = \frac{r_{MO}}{x} - \frac{r_{EX}}{x} \tag{4}$$

where, $\mu_x\left[\frac{1}{h}\right]$ is the specific biomass growth rate; $r_{EX}\left[\frac{g}{L\ h}\right]$ is the manoyl oxide excretion rate; $r_{MO}\left[\frac{g}{L\ h}\right]$ is the manoyl oxide production rate, $Q\left[\frac{L}{h}\right]$ is the medium flow rate, $V_R[L]$ is the total volume of medium in the reactor; $V_{DD}[L]$ is the volume of the dodecane phase in the extraction vessel; $x\left[\frac{g}{L}\right]$ is the biomass concentration in the photobioreactor; $m_{MO}^{X}\left[\frac{g}{g}\right]$ is the concentration of diterpene inside the biomass; $m_{MO}^{AQ}\left[\frac{g}{L}\right]$ is the concentration of diterpene in the medium; $m_{MO}^{DD}\left[\frac{g}{L}\right]$ is the concentration of diterpene in the dodecane phase; and, $K_T\left[\frac{1}{d}\right]$ is a constant related to the liquid-liquid exchange area (a), the mass transfer coefficient (k_T), and the partitioning constant (K_{EQ}).

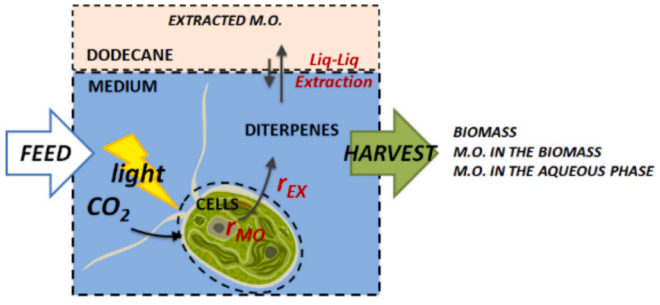

Fig. 3. Schematic representation of the steps involved in the production and extraction of MO from *C. reinhardtii*. MO is produced intracellularly (r_{MO}) and excreted (r_{EX}) to the liquid phase. Once in the aqueous phase, diterpenes are extracted through a liquid-liquid extraction process using dodecane as solvent.

3.2.1. *Effect of cell concentration and light availability on microalgae growth rate*

In a photobioreactor operated under turbidostat control, the biomass specific growth rate (μ_x) can be calculated from the ratio between the flow rate and the reactor volume according to Eq. (1). The biomass productivity (r_X) can then be calculated as the product of the specific growth rate (μ_x) and the biomass concentration (x). Comparing all experimental conditions performed in Infors photobioreactors (Fig. 4), it is possible to observe that the culture with a biomass concentration of 1.37 g l^{-1} reached the highest biomass productivities (r_X) and the highest biomass specific growth rate (μ_X). The lowest biomass productivities reached in the photobioreactor with a biomass concentration of 0.79 g l^{-1} might be related to photosynthetic inhibition inside the reactor, a well described phenomena [23]. On the other hand, at a high biomass concentration (i.e. 2.32 g l^{-1}), the light stratification inside the

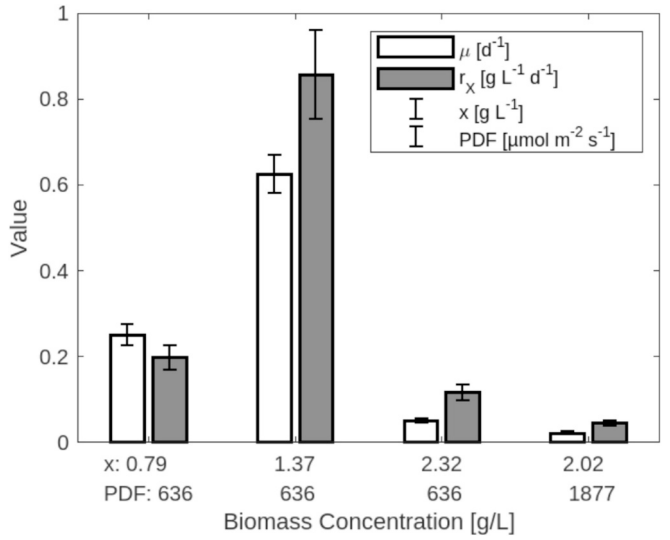

Fig. 4. Biomass volumetric productivity, $r_X\left[\frac{g}{L\,d}\right]$, and microalgae specific growth rate $\mu_X\left[\frac{1}{d}\right]$ in the Infors experiments.

culture and the self-shading effect resulted in a lower light availability for cellular growth. Using those conditions, the specific growth rate (μ_X) and the productivity (r_X) barely exceeded 0.05 d^{-1} and 0.1 g l^{-1} d^{-1}, respectively. Last, increasing the PFD three times (from 636 to 1877 $\mu mol_{ph}\ m^{-2}\ s^{-1}$) did not result in higher biomass productivity but, on the contrary, the biomass production rate turned out to be the lowest.

Results in Fig. 4 showed that under turbidostat conditions, a light intensity of 636 $\mu mol_{ph}\ m^{-2}\ s^{-1}$ positively affected the biomass productivity and the specific growth rate in comparison to 1877 $\mu mol_{ph}\ m^{-2}\ s^{-1}$. The maximum biomass productivity and specific growth rate of 0.85 g l^{-1} d^{-1} and 0.62 d^{-1} was achieved under 636 $\mu mol_{ph}\ m^{-2}\ s^{-1}$ and a biomass concentration in the reactor of 1.37 g l^{-1}.

The specific growth rates (μ) obtained in this work, however, are lower than previous ones reported for *Chlamydomonas reinhardtii* wild type [24,25] but similar to the one previously reported by Lauersen et al. [6].

3.2.2. Effect of cell concentration and light availability on MO production and extraction rates

Photobioreactors experiments in this work were run in turbidostat mode to keep the biomass concentration in the culture constant. However, in a system like the one described in Fig. 3, the concentrations of MO inside the cells (m^X_{MO}), in culture media (m^{aq}_{MO}), and in the dodecane phase (m^{DD}_{MO}) are not necessarily constant. The evolution of MO concentration in the different compartments will be the consequence of four simultaneous processes as described in Fig. 3: the intracellular MO production (r_{MO}); the MO excretion to the aqueous phase (r_{EX}); the rate of MO extraction to the dodecane overlayer ($\frac{dm^{DD}_{MO}}{dt}$); and, the dilution rate of the reactor (Q/V). Changes in the concentration of MO in each phase can be modeled according to Eqs. (2), (3), and (4).

Experimental results showed that the MO concentrations inside the biomass, m^X_{MO}, and in the aqueous phase, m^{AQ}_{MO}, were different in each experimental condition (Table 2); but remained constant over time in all the conditions assayed during the turbidostat control phase (see Fig. 5a). In other words, manoyl oxide did not accumulate in the cells or in the culture media during the continuous phase of cultivation. With that, values of dm^{AQ}_{MO}/dt and dm^X_{MO}/dt in Eqs. (3) and (4) are equal to zero and Eq. (3) can be rearranged as

$$r_{MO} = \frac{Q}{V_R} m^{AQ}_{MO} + \frac{Q}{V_R}\ x\ m^X_{MO} + K_T\ m^{AQ}_{MO} \qquad (3')$$

Table 2
Experimental results for the production and extraction of MO in the Infors photobioreactors.

x $\left[g\ l^{-1}\right]$	PFD $\left[\mu mol\ m^{-2}\ s^{-1}\right]$	dm^{DD}_{MO}/dt $\left[g\ l^{-1}\ d^{-1}\right]$	m^{AQ}_{MO} $\left[g\ l^{-1}\right]$	m^X_{MO} $\left[g\ g^{-1}\right]$	K_T $\left[d^{-1}\right]$
0.79 ± 0.09	636	$1.02 \times 10^{-2} \pm 9{,}0 \times 10^{-4}$	$3.11 \times 10^{-4} \pm 4{,}4 \times 10^{-5}$	$1.54 \times 10^{-3} \pm 3{,}8 \times 10^{-4}$	1.70 ± 0.26
1.37 ± 0.13		$1.24 \times 10^{-2} \pm 1.0 \times 10^{-3}$	$3.30 \times 10^{-4} \pm 3{,}4 \times 10^{-5}$	$4.38 \times 10^{-4} \pm 1{,}0 \times 10^{-4}$	
2.32 ± 0.31		$1.70 \times 10^{-2} \pm 2{,}6 \times 10^{-3}$	$4.51 \times 10^{-4} \pm 1{,}2 \times 10^{-4}$	$4.15 \times 10^{-4} \pm 6{,}2 \times 10^{-5}$	
2.02 ± 0.11	1877	$3.16 \times 10^{-2} \pm 2{,}6 \times 10^{-3}$	$8.76 \times 10^{-4} \pm 0{,}9 \times 10^{-4}$	$1.85 \times 10^{-4} \pm 5{,}2 \times 10^{-5}$	

With this consideration, the model is reduced to Eqs. (1), (2) and (3′). In the model, the values of m^{AQ}_{MO}, m^X_{MO} and x were experimentally measured; V_R, V_{DD} and Q are process parameters; $\frac{dm^{DD}_{MO}}{dt}$ can be calculated from the slope of m^{DD}_{MO} vs. time (see Fig. 5a); and, K_T and r_{MO} can be calculated using Eqs. (2) and (3′) respectively.

The MO concentration in the dodecane phase increases linearly along the time in all assessed conditions. In Fig. 5a $m^{DD}_{MO}(t)$ and $m^{AQ}_{MO}(t)$ are plotted as function of time for the best case scenario for biomass productivity and specific growth rate (1.37 g l^{-1}). This trend is described by Eq. (2), where the term dm^{DD}_{MO}/dt represents the slope of the plot $m^{DD}_{MO}(t)$ *vs* t (MO concentration in the dodecane phase vs time).

When the rate of MO extraction to the dodecane overlayer ($\frac{dm^{DD}_{MO}}{dt}$) is compared the concentration of MO in the aqueous phase (m^{AQ}_{MO}) in the different culture conditions assayed in this research (Fig. 5b), it's observed that the value of $\frac{dm^{DD}_{MO}}{dt}$ increases linearly with the MO concentration m^{AQ}_{MO}. From these results, we can conclude that the use of the first-order equation used in Eq. (2) is consistent with the experimental results. Furthermore, the parameter $K_T\left[\frac{1}{d}\right]$ in the differential equation system can be computed from the slope of Fig. 5 (a) and considering the volumes of the aqueous and dodecane phases according to Eq. (2). The value of $K_T\left[\frac{1}{d}\right]$ is presented in Table 2.

Two important conclusions can be drawn from these results: First, the fact that MO is not accumulated in the biomass implies that m^X_{MO} does not change in time and therefore, MO production rate, r_{MO}, is equal to the MO excretion rate, r_{EX} (Eq. (4)). Second, due to the lack of MO accumulation in the aqueous phase, m^{AQ}_{MO} does not change in time and the total MO produced can be divided in three fractions. These fractions can be identified as separated terms as seen in Eq. (3′): the MO extracted into the dodecane overlayer ($K_T\ m^{AQ}_{MO}$), the MO in the aqueous phase ($Q/V_R m^{AQ}_{MO}$), and the MO inside the cells ($Q/V_R x\ m^X_{MO}$). Thus, it's possible to discern the contribution of these three fractions to the total MO productivity in each experimental set-up (Fig. 6).

From our results, it is possible to see that considering all three experiments at a PFD of 636 [$\mu mol\ m^{-2}\ s^{-1}$] (Fig. 6), the culture conditions with the larger fraction of MO extracted into dodecane corresponds to the higher biomass concentration (2.32 g l^{-1}). However, in these conditions, the total MO produced (this is the addition of the three fractions) was the lowest. On the other hand, the maximum overall MO productivity at a PFD of 636 was reached in the experiment with a biomass concentration of 1.37 g l^{-1} (Fig. 6): 1.20 mg l^{-1} d^{-1}. In this condition,

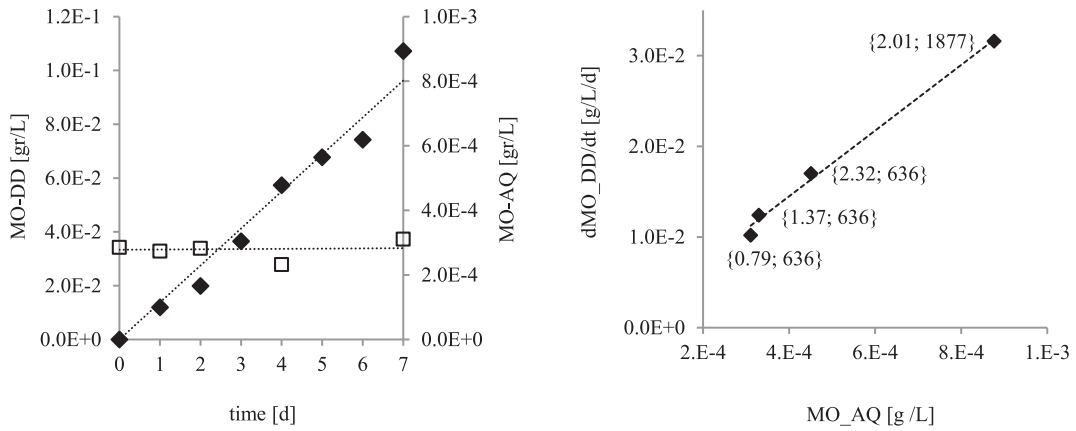

Fig. 5. (a) -(□)- MO concentration in the aqueous phase, $m_{MO}^{aq}(t)$; and, -(◆)- MO concentration in the dodecane phase, $m_{MO}^{DD}(t)$, for the experiment with a biomass concentration of 1,37 [g l^{-1}]. The slope of the plot $m_{MO}^{DD}(t)$ *vs* t correspond to the parameter dm_{MO}^{DD}/dt in Eq. (2). (b) dm_{MO}^{DD}/dt vs $m_{MO}^{DD}(t)$ for all four experiments. Experimental conditions are specified in the plot as {x [gr l^{-1}]; PFD [μmol_{ph} m^{-2} s^{-1}]}.

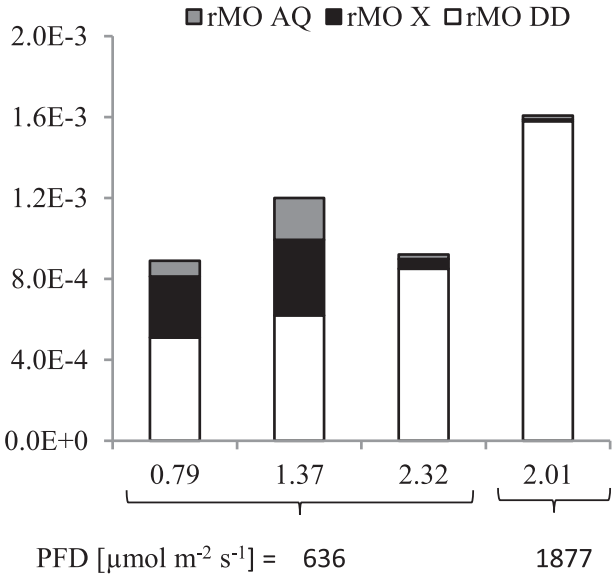

Fig. 6. MO productivities $r_{MO}\left[\frac{g}{L\ d}\right]$ considering the three different fractions: (□) MO in the dodecane phase; (■) in the biomass; and, (■) in the aqueous phase for all culture conditions assayed.

the biomass growth rate was also the highest, resulting in the highest dilution rate. As a consequence, a substantial fraction of the MO was lost in the harvest, either inside the cells (black bars) or in the aqueous phase (gray bars).

When the cultivation was performed using a higher PFD (1877 µmol m^{-2} s^{-1}; 2.01 g l^{-1}), the total amount of MO produced increased 25 % (from 1.20 to 1.60 mg l^{-1} d^{-1}), when compared to the best condition at 636 µmol m^{-2} s^{-1} (biomass concentration = 1.37 g l^{-1}) and up to 50 % (from 0.80 to 1.60 mg l^{-1} d^{-1}) when compared to the others 636 µmol m^{-2} s^{-1} conditions (biomass concentrations = 0.79 and 2.32 g l^{-1} respectively). Although the concentration of MO in the aqueous phase was the highest in that condition, because of the low dilution rate, the fraction of MO extracted in the dodecane was the largest, corresponding to 98 % of the total MO produced. However, our MO titers are slightly lower than those published by Lauersen et al. [6], which may be due to the difference in culture conditions. In their best scenario, a batch cultivation was performed with 3 % CO_2 as a sole source of carbon under a 16:8 light cycle (light intensity 100 µmol m^{-2} s^{-1}), rendering 7 mg MO l^{-1} d^{-1} (vs 1.6 mg MO l^{-1} d^{-1} in our best case). However, it's difficult to theorize and individualize the reasons behind this difference. Aside from the culture conditions, we determined biomass concentration (g l^{-1}) whereas they determined cell density (number cells ml^{-1}), making it more difficult to compare both results.

3.2.3. *Effect of light availability and MO concentration on MO production*

As mentioned before, it's been demonstrated that, if MO is not removed from the culture media, the synthesis of this diterpene is inhibited, hindering the MO production [6]. To analyze the effect of the accumulation of MO in the aqueous phase, we compared the specific MO production rate (Eq. (5)) and the specific light availability (Eq. (6)), together with the aqueous concentration of MO in the PBR experiments (Fig. 7).

$$\mu_{MO}^{sp} = \frac{r_{MO}}{x} \tag{5}$$

$$PFD_{sp}\left[\frac{\mu mol}{g\ s}\right] = PFD\left[\frac{\mu mol}{L\ m^2}\right] \times \frac{Illuminated\ PBR\ area\ [m^2]}{PBR\ volme\ [L]} \times \frac{1}{x\left[\frac{gr}{L}\right]} \tag{6}$$

The variable μ_{MO}^{sp} in Eq. (5) represents the amount of MO produced by

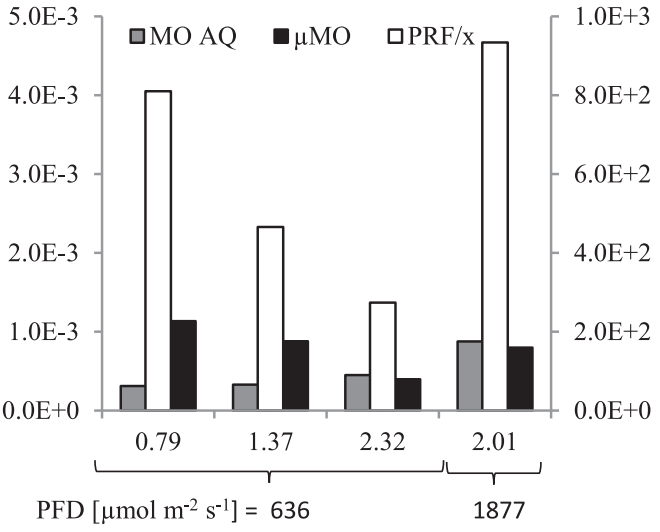

Fig. 7. MO specific productivity, left axis, $\mu_{MO}^{sp}\left[\frac{1}{d}\right]$, (■); MO concentration in the aqueous phase, left axis, $m_{MO}^{aq}\left[\frac{g}{L}\right]$, (■); and, (□) specific photon radiation flux, PFD_{sp} [µmol s^{-1} g^{-1}], right axis, for the four Infors experiments.

the cells. The variable PFD_{sp} in Eq. (6) is related to the amount of light absorbed per gram of biomass in the culture. From these results (Fig. 7), it is possible to reach a better understanding of how light availability and the MO concentration in the aqueous phase influence the overall MO production rate.

When PFD is 636 μmol m^{-2} s^{-1}, the biomass concentration and the aqueous concentration of MO increases simultaneously (gray boxes), whereas, the amount of light absorbed per gram of biomass (white box) and, the amount of MO produced per gram of biomass (black boxes) decreases simultaneously. These results suggest that the reduction in μ_{MO}^{sp} might be the consequence of the reduction in light availability, the accumulation of MO in the medium, or a combination of both variables.

When microalgae were cultured at larger PFD (1877 μmol m^{-2} s^{-1}, biomass concentration of 2.01 g l^{-1}), neither the increase in the aqueous concentration of MO resulted in a proportional reduction of μ_{MO}^{sp} nor the increase in the light availability produced a proportional increase in that value. Although in that condition the amount of light available in the culture PFD was the largest from all four experiments, the amount of MO produced per cell, μ_{MO}^{sp}, was not the maximum. On the other hand, the concentration of MO in the media was the largest in that condition but the amount of MO produced per gram of biomass, μ_{MO}^{sp}, was not the lowest. This result might indicate that both parameters (m_{MO}^{aq} and PFD_{SP}) are simultaneously affecting MO productivity. More light available in the culture stimulates the MO production but, the accumulation of the product in the aqueous phase also inhibits its own synthesis.

According to our results, both light availability and MO accumulation in the aqueous phase are key variables influencing the MO production rate. These factors also affect growth and other cellular processes, highlighting their biological relevance. To better understand their impact, further work is needed to develop models that describe and optimize microalgal growth and MO production kinetics—taking into account both light availability and MO accumulation in the aqueous phase.

3.3. Effect of the extraction area on MO productivity

The analysis of our results suggests that both the accumulation of MO in the aqueous phase and the light availability in the photobioreactor influence the overall MO production and the total amount of MO extracted in the dodecane phase (Figs. 6 and 7). Comparing the MO productivities obtained in flasks and PBRs, it is observed that flasks productivities were significantly higher, despite having lower light availability compared to experiments in photobioreactors.

Aiming at understanding how the extraction capacity of the systems favors the MO production, *C. reinhartii* was cultured in a 0.4 l flat panel photobioreactor (Algaemist Experiments). The difference in extraction capacity between this reactor and the previous PBRs is due to a change in the ratio between the liquid–liquid extraction area and the culture medium volume within the reactor. In this reactor, two different light conditions were tested. The biomass concentration in these experiments was adjusted to reach a similar value of PFD_{SP} in both conditions. Thus, the first experiment was performed at 150 μmol m^{-2} s^{-1} and a biomass concentration of 0.6 g l^{-1}, resulting in a PFD_{SP} of 17.5 [μmol_{PAR} s^{-1} g^{-1}]. The second experiment was performed at 363 μmol m^{-2} s^{-1} and a biomass concentration of 1.29 g l^{-1}, resulting in a PFD_{SP} of 19.67 [μmol s^{-1} g^{-1}]. These values of PFDsp were kept in proximity to allow the assessment of the effect of the surface contact area on the productivity of MO.

In these two experiments, the total MO productivity reached a similar value (2.40 and 2.17 mg $^{-1}$ d^{-1} for the first and second experiment respectively). This outcome was comparable to the results from the Infors reactors, showing that although the amount of light in the Algaemist bioreactors was lower, the MO production was significantly higher. Indeed, under Algaemist conditions, *C. reinhardtii* was able to increase the MO production up to 7.5 times.

The maximum MO productivity obtained in Infors reactors was 1.78 mg l^{-1} d^{-1}; under those conditions, the specific amount of light available, PFD_{SP}, was 43.9 μmol_{PAR} s^{-1} g^{-1}. A greater difference is observed when results in Infors reactor are compared with the experiments in Erlenmeyer flasks. In Erlenmeyer flasks, under a PFD of 318 and 636 μmol_{PAR} m^{-2} s^{-1}, MO productivities were 6.20 and 6.70 mg l^{-1} d^{-1} respectively. Experimental results for all experiments in the three different devices (Erlenmeyer, Infors and Algaemist) are listed in Table 3.

MO productivity in Erlenmeyer reached the maximum values and that increasing the radiation flux from 318 to 636 μmol_{PAR} did not result in a significant increase in the amount of MO produced (Table 3). In Algaemist reactors, MO productivities were lower than the ones in Erlenmeyers and, having almost the same value in the PFD_{SP}, the total MO productivity was similar in both experiments.

The observed differences between the different experiments and light intensities in terms of the MO productivities might be attributed to the extraction capacity of the production system, more specifically, to the extraction area for the dodeacane-media interface in each device. The extraction area is the surface of contact between the culture media and organic phase. The extraction area per culture volume (a [cm^2 l^{-1}] = dodecane contact area [cm^2]/culture volume [L]) can be calculate dividing the contact area and the total culture volume. In Erlenmeyer, the extraction area per culture volume (a) was the largest, with a value of 362.7 cm^2 l^{-1}. When microalgae were cultured under a similar radiation flux (363 μmol m^{-2} s^{-1}), but in Algaemist reactor, there was a 6-time reduction in the extraction area (a = 59.4 cm^2 l^{-1}), and the MO production was significantly reduced. In Infors reactors, the area concentration was the lowest, with a value of 18.7 cm^2 l^{-1} and an additional reduction in the MO productivity was observed. Regardless of the biomass concentration and the radiation flux selected, the values of the r_{MO} in Infors reactors were the lowest among all the experiments even when a PFD of 1877 μmol m^{-2} s^{-1} was used.

Our results, therefore, confirm that the variation in culture conditions has a minor effect on MO production and that the average MO productivity in each reactor linearly increases with the volumetric the extraction area (Fig. 8).

Based on these results, a key conclusion can be drawn: optimizing the extraction capacity of the system is crucial for both the design of the MO production setup and the overall process efficiency.

4. Conclusions

In this work, we showed that the continuous production and simultaneous extraction of MO from *C. reinhardtii* is technologically feasible. The process was demonstrated at bench scale photobioreactors in turbidostat control mode. We evaluated growth and manoyl oxide (MO) production under varying light intensities and analyzed how the system's extraction efficiency impacts MO yields. The highest productivity, 6.7 mg l^{-1} d^{-1}, was achieved in Erlenmeyer flask cultures. While higher light intensity led to slight productivity gains, we observed that although increased light boosts MO production, ineffective extraction significantly limits it, reducing production rates by up to 7.5 times compared to the maximum. These findings indicate that extraction capacity plays a crucial role in optimizing MO production in microalgal cultures, and without effective extraction, additional light availability offers limited benefit to MO productivity. From this work, three key conclusions arise: the accumulation of MO in the aqueous phase and light availability influence the MO production, the main factor determining MO production is the capacity of the production system to remove the diterpene from the aqueous phase, and, the design of the experimental device should assure the efficient removal of the produced diterpene.

CRediT authorship contribution statement

Josué M. Heinrich: Writing – review & editing, Writing – original

Table 3
Experimental results for the production and extraction of MO in the different devices.

Operation mode	Experiment set-up	PFD $\left[\frac{\mu mol}{s\ m^2}\right]$	Biomass $\left[\frac{g}{l}\right]$	a $\left[\frac{cm^2}{l}\right]$	r_X $\left[\frac{g}{l\ d}\right]$	PFD_{SP} $\left[\frac{\mu mol}{g\ s}\right]$	r_{MO} $\left[\frac{mg}{l\ d}\right]$
Batch	Erlenmeyer	318	0.1 to 1.8	362.7	0.33	var.	6.20
		636	0.1 to 1.8		0.30	var.	6.70
Continuous	Algemist	150	0.60	59.4	0.36	17.5	2.40
		363	1.29		n.d.	19.67	2.17
	Infors	636	0.79	18.7	0.20	37.84	0.89
			1.37		0.85	21.81	1.20
			2.32		0.12	12.88	0.92
		1877	2.01		0.33	43.90	1.78

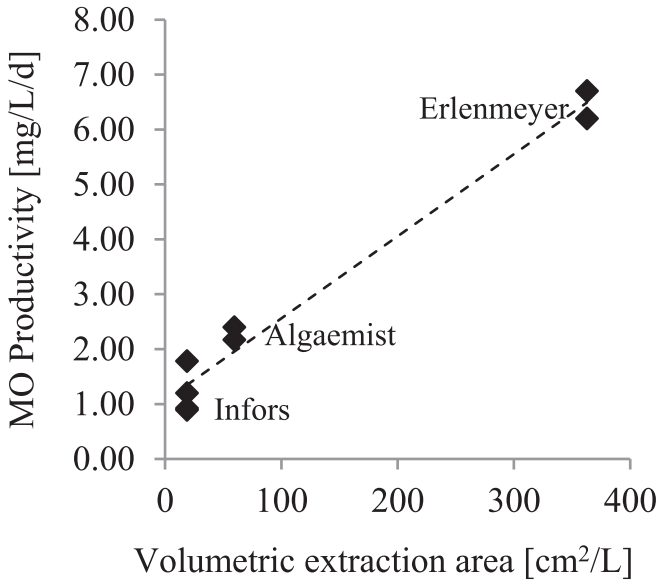

Fig. 8. MO productivity, $r_{MO}\left[\frac{mg}{L\ d}\right]$ vs volumetric extraction area [$cm^2\ l^{-1}$] considering all experiments in Erlemeyer flasks, Algaemist and Infors reactors.

draft, Supervision, Funding acquisition, Conceptualization. **Iago Teles Dominguez Cabanelas:** Writing – original draft, Supervision, Investigation, Conceptualization. **Sara S. Cidraes Vieira:** Methodology, Formal analysis, Conceptualization. **Rafael García-Cubero:** Writing – review & editing, Writing – original draft. **María J. Barbosa:** Writing – review & editing, Resources, Funding acquisition. **René H. Wijffels:** Writing – review & editing, Resources, Funding acquisition.

Declaration of competing interest

The authors declare the following financial interests/personal relationships which may be considered as potential competing interests: Josue Heinrich reports financial support was provided by ERA-Net Cofund scheme. Rene Wijffels reports financial support was provided by ERA-Net Cofund scheme. If there are other authors, they declare that they have no known competing financial interests or personal relationships that could have appeared to influence the work reported in this paper.

Acknowledgements

The authors would like to express thanks to Kyle J. Lauersen for providing strain *Chlamydomonas reinhardtii* (B2). This work was financially supported by the grant agreement No. 722361, from the program ERA CoBioTech, an ERA-Net Cofund Action under the European Union's Horizon 2020 research and innovation programme (H2020).

Data availability

Data will be made available on request.

References

[1] B.M. Lange, T. Rujan, W. Martin, R. Croteau, Isoprenoid biosynthesis: the evolution of two ancient and distinct pathways across genomes, Proc. Natl. Acad. Sci. U. S. A. 97 (2000) 13172–13177, https://doi.org/10.1073/pnas.240454797.
[2] J. Bohlmann, C.I. Keeling, Terpenoid biomaterials, Plant J. 54 (2008) 656–669, https://doi.org/10.1111/j.1365-313X.2008.03449.x.
[3] M.D. Leavell, D.J. McPhee, C.J. Paddon, Developing fermentative terpenoid production for commercial usage, Curr. Opin. Biotechnol. 37 (2016) 114–119, https://doi.org/10.1016/j.copbio.2015.10.007.
[4] A. Caniard, P. Zerbe, S. Legrand, A. Cohade, N. Valot, J.-L. Magnard, J. Bohlmann, L. Legendre, Discovery and functional characterization of two diterpene synthases for sclareol biosynthesis in Salvia sclarea (L.) and their relevance for perfume manufacture, BMC Plant Biol. 12 (2012) 119, https://doi.org/10.1186/1471-2229-12-119.
[5] U. Christensen, D. Vazquez-Albacete, K.M. Søgaard, T. Hobel, M.T. Nielsen, S. J. Harrison, A.H. Hansen, B.L. Møller, S. Seppälä, M.H.H. Nørholm, De-bugging and maximizing plant cytochrome P450 production in Escherichia coli with C-terminal GFP fusions, Appl. Microbiol. Biotechnol. 101 (2017) 4103–4113, https://doi.org/10.1007/s00253-016-8076-5.
[6] K.J. Lauersen, J. Wichmann, T. Baier, S.C. Kampranis, I. Pateraki, B.L. Møller, O. Kruse, Phototrophic production of heterologous diterpenoids and a hydroxy-functionalized derivative from Chlamydomonas reinhardtii, Metab. Eng. 49 (2018) 116–127, https://doi.org/10.1016/j.ymben.2018.07.005.
[7] J. Ruiz, G. Olivieri, J. De Vree, R. Bosma, P. Willems, J.H. Reith, M.H.M. Eppink, D. M.M. Kleinegris, R.H. Wijffels, M.J. Barbosa, Towards industrial products from microalgae, Energ. Environ. Sci. 9 (2016) 3036–3043, https://doi.org/10.1039/c6ee01493c.
[8] R.H. Wijffels, M.J. Barbosa, An outlook on microalgal biofuels, Science 329 (2010) 796–799, https://doi.org/10.1126/science.1189003.
[9] R. García-Cubero, W. Wang, J. Martín, E. Bermejo, L. Sijtsma, A. Togtema, M. J. Barbosa, D.M.M. Kleinegris, Milking exopolysaccharides from Botryococcus braunii CCALA778 by membrane filtration, Algal Res. 34 (2018) 175–181, https://doi.org/10.1016/J.ALGAL.2018.07.018.
[10] D.M.M. Kleinegris, M. Janssen, W.A. Brandenburg, R.H. Wijffels, The selectivity of milking of *Dunaliella salina*, Marine Biotechnol. 12 (2010) 14–23, https://doi.org/10.1007/s10126-009-9195-0.
[11] M.A. Hejazi, C. De Lamarliere, J.M.S. Rocha, M. Vermuë, J. Tramper, R.H. Wijffels, Selective extraction of carotenoids from the microalga Dunaliella salina with retention of viability, Biotechnol. Bioeng. 79 (2002) 29–36, https://doi.org/10.1002/bit.10270.
[12] S.K. Satpute, A.G. Banpurkar, P.K. Dhakephalkar, I.M. Banat, B.A. Chopade, Methods for investigating biosurfactants and bioemulsifiers: a review, Crit. Rev. Biotechnol. 30 (2010) 127–144, https://doi.org/10.3109/07388550903427280.
[13] J.T. Tuttle, J.R. Williams, D.C. Higgs, Characterization of a Chlamydomonas reinhardtii mutant strain with tolerance to low nitrogen and increased growth and biomass under nitrogen stress, Algal Res. 50 (2020), https://doi.org/10.1016/j.algal.2020.102000.
[14] R. García-Cubero, W. Wang, J. Martín, E. Bermejo, L. Sijtsma, A. Togtema, M. J. Barbosa, D.M.M. Kleinegris, Milking exopolysaccharides from Botryococcus braunii CCALA778 by membrane filtration, Algal Res. 34 (2018) 175–181, https://doi.org/10.1016/j.algal.2018.07.018.
[15] K.J. Lauersen, T. Baier, J. Wichmann, R. Wördenweber, J.H. Mussgnug, W. Hübner, T. Huser, O. Kruse, Efficient phototrophic production of a high-value sesquiterpenoid from the eukaryotic microalga Chlamydomonas reinhardtii, Metab. Eng. 38 (2016) 331–343, https://doi.org/10.1016/J.YMBEN.2016.07.013.
[16] R. García-Cubero, D.M.M. Kleinegris, M.J. Barbosa, Predicting biomass and hydrocarbon productivities and colony size in continuous cultures of Botryococcus braunii showa, Bioresour. Technol. 340 (2021), https://doi.org/10.1016/j.biortech.2021.125653.
[17] Z. Huang, L. Shen, W. Wang, Z. Mao, X. Yi, T. Kuang, J.-R. Shen, X. Zhang, G. Han, Structure of photosystem I-LHCI-LHCII from the green alga Chlamydomonas

reinhardtii in state 2, Nat. Commun. 12 (2021), https://doi.org/10.1038/s41467-021-21362-6.
[18] J. Legrand, A. Artu, J. Pruvost, A review on photobioreactor design and modelling for microalgae production, React. Chem. Eng. 6 (2021) 1134–1151, https://doi.org/10.1039/d0re00450b.
[19] S. Najiha Badar, M. Mohammad, Z. Emdadi, Z. Yaakob, Algae and their growth requirements for bioenergy: a review, Biofuels 12 (2021) 307–325, https://doi.org/10.1080/17597269.2018.1472978.
[20] D.M.M. Kleinegris, M. Janssen, W.A. Brandenburg, R.H. Wijffels, Continuous production of carotenoids from Dunaliella salina, Enzyme Microb. Technol. 48 (2011) 253–259, https://doi.org/10.1016/j.enzmictec.2010.11.005.
[21] R. García-Cubero, I.T.D. Cabanelas, L. Sijtsma, D.M.M. Kleinegris, M.J. Barbosa, Production of exopolysaccharide by Botryococcus braunii CCALA 778 under laboratory simulated Mediterranean climate conditions, Algal Res. 29 (2018) 330–336, https://doi.org/10.1016/j.algal.2017.12.003.
[22] P.C. Oostlander, J. van Houcke, R.H. Wijffels, M.J. Barbosa, Growth and fatty acid content of Rhodomonas sp. under day:night cycles of light and temperature, Algal Res. 51 (2020), https://doi.org/10.1016/j.algal.2020.102034.
[23] T. Roach, A. Krieger-Liszkay, Regulation of photosynthetic electron transport and photoinhibition, Curr. Protein Pept. Sci. 15 (2014) 351–362, https://doi.org/10.2174/1389203715666140327105143.
[24] T. de Mooij, G. de Vries, C. Latsos, R.H. Wijffels, M. Janssen, Impact of light color on photobioreactor productivity, Algal Res. 15 (2016) 32–42, https://doi.org/10.1016/j.algal.2016.01.015.
[25] J. Hahm, A. Bauer, S.-H. Jung, N. Zell, F. Boßle, R. Buchholz, C. Lindenberger, Process parameter screening for the microalga Chlamydomonas asymmetrica in batch and turbidostat cultivations, Chemie-Ingenieur-Technik 93 (2021) 1565–1572, https://doi.org/10.1002/cite.202100046.
[26] Y. Liu, C. Xixian, Z. Congqiang, Sustainable biosynthesis of valuable diterpenes in microbes, Eng. Microbiol. 3 (1) (2023) 100058, https://doi.org/10.1016/j.engmic.2022.100058.